ENGINEER - Vol. LVIII, No. 03, pp. [53-66], 2025

DOI: https://doi.org/10.4038/engineer.v58i3.7704

Statistical Approach to Selecting Global Circulation Models (GCMs) – A Study Based in the Kalu Ganga Catchment of Sri Lanka

Mananjaya Balasooriya and Panduka Neluwala

Abstract: This study proposes a two-stage Global Circulation Model (GCM) selection approach that evaluates the performance of CMIP5 GCMs in simulating past rainfall for the Kalu Ganga catchment in Sri Lanka. In the initial selection, GCMs were screened based on their ability to replicate monsoonal rainfall patterns using data from the Global Precipitation Climatology Project (GPCP). The fine selection involved bias-corrected GCM simulations at the catchment scale across three rainfall categories—extreme events, normal rainfall, and no-rain days—validated against the Asian Precipitation Highly Resolved Observational Data Integration Towards Evaluation (APHRODITE) dataset. Several statistical performance indicators (PIs) were used to assess GCM performance at both stages, and Multi-Criteria Decision-Making (MCDM) techniques were applied to rank the GCMs accordingly. The results indicated that CanESM2 is most suitable for simulating extreme rainfall events, CNRM-CM5 for normal rainfall, and either CanESM2 or CNRM-CM5 for no-rain days. This highlights that no single GCM performs optimally across all rainfall categories, and researchers should select GCMs tailored to their specific focus on future rainfall extremes, flood risk, or drought analysis.

Keywords: Climate Change, Kalu Ganga, APHRODITE, GPCP, GCM Selection, Bias Correction

1. Introduction

The adverse effects of climate change are numerous, including global warming, changes in hydrological systems, alterations in crop yields, and impacts on animal species' habitats [40]. These macroscopic climate changes could affect the hydrological regime at the catchment level [33]. To study the foreseeable impacts of such climate change, it is essential to have an understanding of future rainfall projections that could lead to devastating floods [37]. Global Circulation Models (GCMs) are used as tools to forecast future climatic parameters, such as rainfall [13, 23]. The Coupled Model Intercomparison Project Phase 5 (CMIP5), developed for the Intergovernmental Panel on Climate Change (IPCC), has brought together more than sixty different GCMs designed to generate future climate parameters to support sustainable climate resilience decisions [32]. With the limitations of the available data in mind, a suitable GCM or ensemble of GCMs should be used to conceptualize the hydrological impacts within the local context [34]. Selecting an appropriate GCM from the CMIP5 ensemble is challenging, given their limitations in geophysical accuracy when applied to regions other than those for which the models were originally developed. On the other hand, selecting an appropriate GCM to model regional climatic parameters is essential for catchment-level studies [14, 24].

Using ensembles of GCMs could be an alternative to selecting a single GCM, but it is generally better to choose a suitable GCM capable of modelling past rainfall [35]. A few studies in the South Asian region involving GCM simulations have selected GCMs based on the availability of comprehensive datasets relevant to their specific modelling objectives [7,11, 22, 29], while other studies have selected GCMs based on their ability to reproduce meteorological parameters accurately [20, 24].

The ability of GCMs to simulate past rainfall and temperatures has been evaluated using performance indicators [7, 26], and various methods have been employed to rank GCMs based on their performance according to these indicators [34]. Each performance indicator has its own inherent strengths and weaknesses; as a result, the evaluation criteria of GCM performance differ among indicators. For example, using a single performance indicator for an absolute comparison between two variables is unacceptable. The ranking methods used in GCM selection studies range from simple to statistically advanced, often involving multiple stages of calculation [14]. In addition, the selection of GCM under different criteria with mean and projected extreme rainfalls has been attempted [17].

Eng. Mananjaya Balasooriya, AMIE(SL), GMICE(UK), M.Sc. Eng, B.Sc. Eng. (Peradeniya), Civil Engineer, National Water Supply and Drainage Board. Email:eng.mananjaya@gmail.com
https://orcid.org/0009-0002-5587-2634 **Eng. (Dr.) Panduka Neluwala**, AMIE(SL), B.Sc. Eng. (Peradeniya), M.Eng., Ph.D. (Tokyo), Senior Lecturer, Dept. of Civil Engineering, University of Peradeniya, Sri Lanka. Email:pandukaneluwala@eng.pdn.ac.lk
https://orcid.org/0000-0002-1686-3412

When GCMs are selected based on their ability to model the past, the use of past climatological data is often required in the assessment of a GCM's performance [17]. The use of gridded rainfall data could minimize the data cost but does not compromise the pool of data that can be accessed [3, 26]. APHRODITE rainfall data is made from ground observation rainfall records, and on the grid scale, Sri Lanka belongs to the Monsoonal Asia subdomain and has rainfall data at 0.25° grid intervals [38]. APHRODITE has been proven to be a better gridded rainfall dataset in parts of South-East Asia [23] and most of the Asian region except the Tibetan plateau [31], but evidence of its use for studies in Sri Lanka is lacking. In contrast, GPCP data has both land and ocean coverage due to its ability to reproduce satellite data inputs into gridded precipitation; as a result, a larger area for small islands comprising land and its surrounding ocean can be used for analysis [1].

CMIP5 web index is commonly used in studies as the source of GCM simulations [7, 11, 35]. Data Integration and Analysis System (DIAS) is an online application which can be used to obtain GCM simulations [32], where the GCM simulations can be compared with historical reference data, thus enabling GCM selection to be easier for the intended region without the need to download and process large datasets [24]. DIAS-CMIP5 uses bias correction based on rainfall classification into extreme, normal, and wet day rainfalls [32], since raw GCM projections would not be ideal for comparison with observed data as these could deviate due to systematic errors and deficient geophysical characteristics included during their development stages [21, 44]. This makes bias correction of GCM projections an integral part of climate change and impact analysis since GCM outputs are unmatched at the local scale by their nature [16]. In contrast to dynamic methods, statistical downscaling can reasonably preserve spatial and temporal relationships over a region since the downscaling approach is based on historical observations [24]; when historical climatological parameters are used for downscaling, this approach can be used as a method of bias correction in GCM outputs [30]. Compared to other statistical techniques, the quartile-based mapping method on cumulative distribution functions has been tested and used in many studies as a robust method of bias correction [10, 15, 44].

Based on the bias correction method developed under DIAS, this study categorizes rainfall as Wet Day Rainfall (WDR), No Rainy Days (NRD), and Extreme Rainfall Events (ERE) using rainfall thresholds. WDR is defined as normal rainfall received between the extreme rainfall and no rain thresholds, excluding extreme events and dry days of a particular month. Thevakaran [27] stated that the 99th percentile of each year's rainfall distribution would be more appropriate for defining extreme rainfall, and a minimum crop water demand of 1 mm could be the threshold for no rain. Burt and Weerasinghe [6] identified a minimum of 5 mm of rainfall for a wet day. However, using a fixed rainfall value as the minimum threshold to split wet and dry days would not be ideal for a GCM-simulated distribution since these distributions carry bias along with distorted distributions after simulations.

It is seen that most GCM-based studies in the region focus on selecting one GCM without attempting to identify whether the selected GCM can model future rainfall more precisely in the three rainfall categories identified above. The results of this study can be used to distinguish whether differentiation of GCMs is required when modelling extreme and normal rainfalls and no rain days or whether a single GCM could accommodate all three rainfall categories in the catchment of interest. This would enable researchers to prepare for more accurate rainfall modelling in climate studies, such as floods or droughts. In addition, several studies have attempted to establish the possible impacts of climate change on major river basins in Sri Lanka but used arbitrarily chosen GCMs from the CMIP archive [8, 42, 43], while a few other studies also developed GCM selection methods [20, 24]. In contrast, this study proposes a two-stage GCM selection method based on gridded precipitation data intended for the Kalu Ganga basin, one of the most heavily flooded zones [9, 19] in Sri Lanka during abnormal monsoon periods. The proposed methodology can also be applied to other catchments with appropriate modifications.

2. Methodology

The initial selection was based on the GCMs' applicability to the monsoonal rainfall pattern, followed by the fine selection based on catchment-level rainfall. For the latter, the rainfalls were categorized and bias-corrected accordingly, prior to the analysis to enable different comparisons among the three categories. Since the GCM selection was based on gridded precipitation, spatial and temporal data availability was critical in both the initial and fine selections. The DIAS platform (http://www.diasjp.net/) was used to obtain the GCM simulations of observed past rainfall, while the historical daily rainfall data for the study area were obtained from GPCP for the period 1979–2005 and from APHRODITE for the period 1981–2001. The process is given in the flow diagram shown in Figure 1.

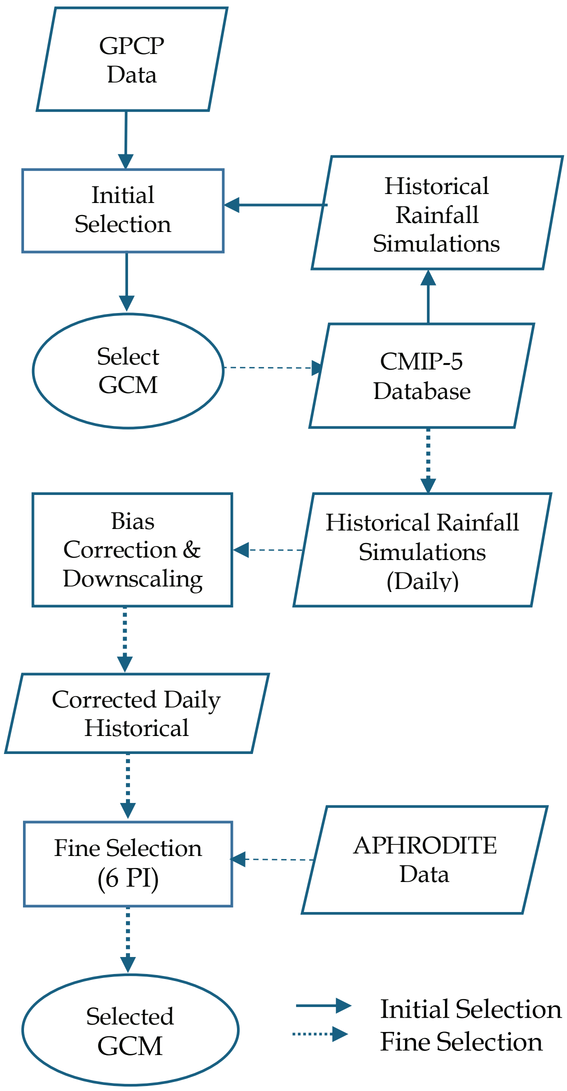

Figure 1 - Process Flow Chart

2.1 Initial Selection

Based on the temporal monthly distribution of rainfall in the southwestern part of the island due to the monsoonal climate, an obvious pattern was identified and used as the basis for the initial selection. The monthly rainy periods were classified as Wet, Dry, Wet-Intermediate, and Dry-Intermediate months.

- Peaks in May and October (Wet Months)
- Troughs in February and August (Dry Months)
- Rising – March & April, September (Wet-Intermediate Months)
- Declining – June & July, November-January (Dry-Intermediate Months)

To demonstrate this monsoonal rain pattern, the initial selection was carried out for the region encompassing the island surrounded by the Indian Ocean, including a larger domain bounded by (79°E, 5.5°N), (81.5°E, 5.5°N), (76.5°E, 8°N), and (81.5°E, 8°N), as shown in Figure 2.

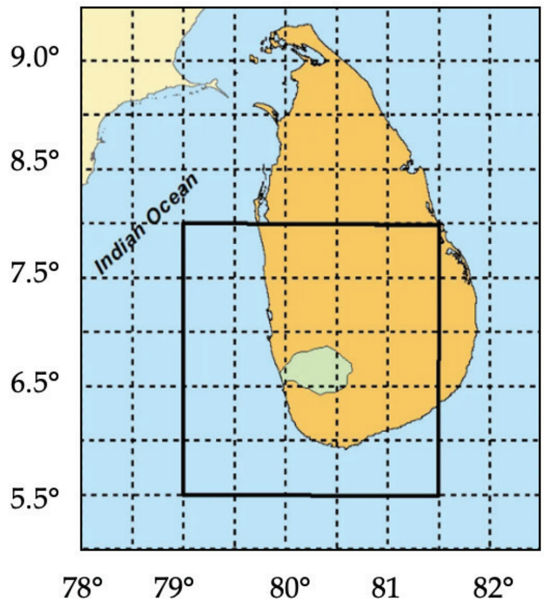

Figure 2 - Initial Selection Grids

Since this selection included an area comprising both land and ocean, GPCP precipitation data were used as the observed dataset [22, 24]. Monthly precipitation data from GPCP forÍ the intended area spanned from 1979 to 2005.Historical simulations of precipitation by different CMIP5 GCMs for the period 1979 to 2005 and observed rainfall (GPCP) datasets were compared for their compatibility using two statistical Performance Indicators (PIs) given as Eq. 1 and Eq. 2 under the eight individual monthly periods identified above (May, October, August, February, March-April, September, June-July, November -January).

Root Mean Square Error

$$RMSE = \sqrt{\frac{1}{N}\sum_{1}^{N}(x_i - y_i)^2} \qquad \ldots(1)$$

Spatial correlation coefficient

$$Scorr = \frac{\sum_{1}^{n}(x_i - \bar{x})(y_i - \bar{y})}{\sqrt{\sum_{1}^{n}(x_i - \bar{x})^2 (y_i - \bar{y})^2}} \qquad \ldots(2)$$

where x_i and y_i are the two variables, while $\bar{x}$ and $\bar{y}$ resemble their means. Based on the RMSE and Scorr values obtained by each GCM, a filtering criterion was introduced such that a particular GCM would receive.

- a mark of 1 if and only if
  RMSE <= RMSE_Average and
  Scorr>= Scorr_Average,
- a mark of -0.5 if and only if
  RMSE >RMSE_Average and
  Scorr<Scorr_Average,

In all other cases, the mark was 0. This criterion was applied to all eight predefined time periods of monthly rainfall variation patterns. The marks for each GCM across all eight comparison steps were summed to obtain a final score out of eight. Based on this, the GCMs were ranked such that those with higher scores received higher rankings. GCMs that obtained a mark of 1 in at least three criteria were initially selected to proceed to the fine selection.

2.2 Fine Selection

The extent of the land mass of Sri Lanka is small, but there is a high spatial and temporal variation of precipitation [36]. The GPCP data availability is in 2.5° grid intervals which can include half of the island's land mass (Figure 2). Therefore, a further step of fine selection was needed that can possibly demonstrate catchment specific rainfall outputs. The analysis area of the Fine Selection process is shown in Figure 3. Six grid points at 0.25° interval were selected as the representative area of the catchment.

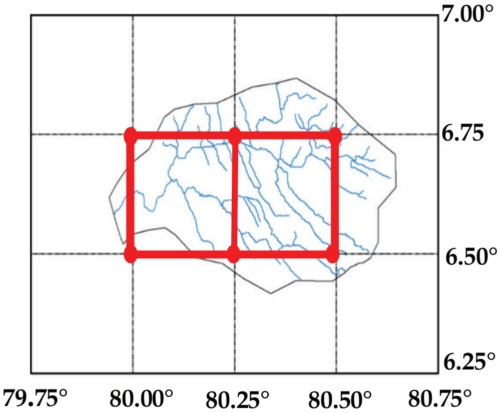

Figure 3 - Fine Selection Grid

Fine selection of GCM together with the bias correction is executed under three rainfall categories such that Extreme Rainfall Events (ERE), Wet Day Rainfall (WDR), No Rain Days (NRD) based on set thresholds. A percentile figure of 50% was set as the minimum rainfall in which this criterion is further supported in the propensity that as an average, Kalu Ganga basin is in wet condition for a half year period. In determining the extreme precipitation threshold, the 99th percentile is adopted where it was determined out of the total dataset of the analysis period (i.e., out of the whole 20 years daily rainfall). The daily rainfalls in between the 99th and the 50th rainfalls of each simulated past and observed past rainfalls were treated as WDR. Rainfalls above the 99th percentile and below the 50th percentile of each simulated past and observed past rainfalls were treated as ERE and NRD, respectively.

From AHRODITE data, daily precipitations at 0.25° grid intervals were obtained as the observed dataset. The historical simulations of CMIP5-DIAS are limited to the period from 1981 to 2000 hence the analytical period was set to 20 years. A statistical method of GCM selection was developed in this study with the aid of previous studies [25] which could be used for other catchments as well.

The APHRODITE precipitation at one grid point could be based on nearby in-situ precipitation data stations with computations and absence of rainfall records marked as zero rain days. Therefore, to overcome this nature of uncertainty the gridded rainfall data is averaged and taken as the representative for the entire catchment to be used in the GCM selection and further analysis steps. However, for extreme rainfall events the highest rainfalls from each grid point of the catchment were taken into consideration in order to avoid the extreme rainfalls being underestimated when averaged.

2.2.1 Bias Correction of GCM Rainfall

The bias correction was done with respect to the previously identified three rainfall categories. For the bias correction step, a few changes were adopted in this study compared to previous studies [20]. These included the summing of WDR to obtain Monthly Wet Day Rainfall (MWDR), and the introduction of percentile thresholds to select extreme events and no-rain days. The latter helped to ensure that the number of dry days and the number of extreme events for the respective periods were kept equal between the observed and simulated datasets.

2.2.1.1 Extreme Rainfall ERE Bias Correction

The Generalized Pareto Distribution (GPD) is widely used in modelling the tails of rainfall series. In this study, the extreme events of the observed past and simulated past were modelled using the same. The GPD parameters were calculated separately for these two distributions of extreme rainfall. Then, extreme rainfall bias correction was applied using the Quantile-Based Mapping method, as given by the following Eq. (03) [10,44].

$$X_{GCM\_Corr} = F_{Obs}^{-1}\left(F_{GCM}(x)\right) \qquad \ldots(3)$$

X_{GCM_Corr} is the bias-corrected rainfall and x is the GCM simulated rainfall. F and F^{-1} are the CDF and inverse CDF respectively where the subscripts Obs and GCM represent the observed and GCM simulated subsets, respectively.

2.2.1.2 No Rain Days Correction

In the GCM-simulated rainfall data for the historical period, a large number of rainy days with low rainfall magnitudes were observed.

This tendency is likely due to the detailed parameterization schemes used in GCM simulations [20]. To address this issue, simulated daily rainfall values below the 50th percentile (i.e., the no-rain day threshold) of the observed daily rainfall distribution were set to zero.

2.2.1.3 Wet Day Rainfall Correction
The Gamma distribution, given by Eq. (4), which is widely used to model monthly rainfall distributions [12,18], was employed to model the Monthly Wet Day Rainfalls (MWDR) in this study as well. Similar to the bias correction applied to extreme rainfall using Eq. (3), the historical simulations of MWDR were bias corrected accordingly.

2.2.2 Comparison Analysis
The performance indicators given by Eqs. (4)–(9) were used to evaluate the relationship between the observed rainfall and the GCM-simulated, bias-corrected historical rainfall in a head-to-head comparison.

Normalized Root Mean Square Error

$$RMSD = \frac{\sqrt{\frac{1}{n}\sum_1^n (x_i - y_i)^2}}{\bar{x}} \quad \dots (4)$$

Average Absolute Relative Deviation

$$AARD = \frac{1}{n}\sum_1^n \left|\frac{y_i - x_i}{x_i}\right| \quad \dots (5)$$

Absolute Normalized Mean Bias Deviation

$$ANMBD = \left|\frac{\frac{1}{n}\sum_1^n (y_i - x_i)}{\bar{x}}\right| \quad \dots (6)$$

Nash-Sutcliffe Efficiency Coefficient

$$NSE = 1 - \frac{\sum_1^n (x_i - y_i)^2}{\sum_1^n (x_i - \bar{x})^2} \quad \dots (7)$$

Pearson Correlation Coefficient

$$CC = \frac{\sum_1^n (x_i - \bar{x})(y_i - \bar{y})}{(n-1)\sigma_{obs}\sigma_{sim}} \quad \dots (8)$$

Skill Score

$$SS = \frac{1}{n}\sum_1^n \min(f_0, f_s) \quad \dots (9)$$

where x_i and y_i are the two variables, while $\bar{x}$ and $\bar{y}$resemble the mean of the two variables. $\sigma_{obs} and \sigma_{sim}$ are the standard deviations of the observed and simulated variables. f_0, and f_s are the frequencies of observed and simulated variables in the groups of data.

Four out of the six performance indicators (Eqs. 5–8) are measures of the deviations of the simulated rainfall values from the observed rainfall data. Both NRMSD and AARD quantify the magnitude of these deviations, while ANMBRD measures the direction of the deviations. NSE represents the ratio between two deviations. The Pearson Correlation Coefficient (CC) evaluates the strength of the linear relationship between the simulated and observed rainfall, whereas the Skill Score (SS) compares the probability distributions of the two rainfall variables. For NRMSD, AARD, and ANMBRD, lower values indicate better performance, while for NSE, CC, and SS, higher values closer to 1 are preferred.

The rainfall comparison was conducted at the monthly scale to reduce the variability inherent in daily rainfall data. Specifically, the sums of extreme events, daily rainfall amounts, and the number of no-rain days within each month were compared between the observed and GCM-simulated datasets for each GCM screened during the initial selection.

If T GCMs were screened by the initial selection, and L performance indicators were used to evaluate their ability to simulate past rainfall, this would result in a T × L matrix containing numerous data points for analysis in the Fine Selection process. Therefore, to simplify the calculation process and rank the GCMs based on their performance, an appropriate method was required to aid the decision-making process for selecting better-performing models. Multi-Criteria Decision Making (MCDM) techniques were therefore employed to generate a single rank for each GCM based on their performance indicators [25].

Applying these performance indicators within a single function, i.e. using MCDM equations to rank the GCMs requires assigning weighted averages to each indicator. The weights for each performance indicator were calculated using the Entropy method, as described by Eqs. 10–13 [25].

The normalized value of indicator 'j' for GCM 'a'

$$k_{aj} = \frac{k_j(a)}{\sum_1^T k_j(a)} \quad \dots (10)$$

The entropy value of indicator 'j'

$$En_j = -\frac{1}{\ln(T)}\sum_1^T k_{aj}.\ln(k_{aj}) \quad \dots (11)$$

Degree of diversification

$$Dd_j = 1 - En_j \quad \dots (12)$$

Normalized weight of indicator

$$r_j = \frac{Dd_j}{\sum_1^n Dd_j} * 100\% \quad \dots (13)$$

where 'T' is the number of GCMs used for analysis while 'n' is the number of indicators used for the analysis. Two different MCDM techniques were used to evaluate whether both the methods portray the same results.

2.2.2.1 Compromise Linear Programming (CP)

A specialized distance function was used to calculate the resultant distance of each performance indicator from its ideal solution [25]. This distance is minimized when the performance indicators are closer to their ideal values. The distances denoted by L_{pa} were computed using Eq. 14 for each GCM, and the GCMs were ranked accordingly, with the lowest L_{pa} value receiving the highest rank.

$$L_{pa} = \left(\sum_{j=1}^{J} r_j^{p} \left|k_j(a) - k_j\right|^{p}\right)^{\frac{1}{p}} \quad \text{... (14)}$$

where L_{pa} – Distance Measure Matrix of GCM a, j – Number of indicators, r_j– Weight assigned to the indicator j, $k_j(a)$–Normalized value of indicator j for GCM a, k_j– Normalized optimal solution to the original problem, p - Parameter (1, 2, …∞).

The performance indicators NSE, CC, and SS have an ideal value of 1, whereas RMSD, NRMSD, AARD, and ANMBD do not have predefined ideal values. For these indicators, the lowest value among the calculated results was considered as the ideal solution, based on the rationale that the decision-maker can define a reference or ideal value [41]. In this context, the deviation-based performance indicators (RMSD, NRMSD, AARD, and ANMBD) were transformed into their negative values, as the compromise programming technique required to identify the maximum value for each indicator as the ideal solution.

2.2.2.2 Technique for Order Preference by Similarity to an Ideal Solution (TOPSIS)

This technique evaluates both the distance to the ideal solution (Proximal Distance) and the distance from the anti-ideal solution (Separation Distance). The resulting value is expressed as the Relative Closeness of a model to its optimal solution. The underlying principle is that the optimal solution should have the shortest distance to the ideal solution and the greatest distance from the anti-ideal solution [39]. The two Separation Distance matrices and the resulting Relative Closeness values were calculated for all GCMs, and the models were ranked based on their CR_a values, with the highest CR_a receiving the highest rank.

Relative Closeness

$$CR_a = \frac{DS_a^-}{(DS_a^+ + DS_a^-)} \quad \text{...(15)}$$

Separation Distance

$$DS_a^+ = \sqrt{\sum_{j=1}^{j} r_j (K_j(a) - K_j^*)^2} \quad \text{... (16)}$$

$$DS_a^- = \sqrt{\sum_{j=1}^{j} r_j (K_j(a) - K_j^{**})^2} \quad \text{... (17)}$$

where DS_a^+ - Distance matrix relative to the ideal solution, DS_a^- - Distance matrix relative to the anti-ideal solution, K_j^*–Normalized optimal solution to the original problem, K_j^{**}- Normalized anti-ideal solution to the original problem and the other symbols are as defined previously.

2.2.2.3 Group Decision Making

If the two MCDM techniques ranked the GCMs in different orders, a Group Decision-Making (GDM) approach was applied to derive a final ranking [25]. A similar approach has been followed using the frequency of occurrence method [11].

The rankings from the two MCDM techniques were analysed using the Group Decision-Making (GDM) approach, and the Net Strength(NS_a) values were calculated for all seven GCMs. This procedure was repeated for each rainfall category. Higher Net Strength (NS_a) indicates suitable GCM.

Strength of GCM 'a'

$$St_a = \sum_{k=1}^{m} \sum_{z}^{x} (X - z + 1)\ q_{az}^{k} \quad \text{... (18)}$$

Weakness of a GCM 'a'

$$We_a = \sum_{k=1}^{m} \sum_{z}^{x} (z - Y + 1)\ q_{az}^{k} \quad \text{... (19)}$$

Net Strength of a GCM

$$NS_a = St_a - We_a \quad \text{... (20)}$$

$$X = \begin{cases} \frac{T}{2}\ ; & T \text{ is an even number} \\ \frac{T}{2} + 1\ ; & T \text{ is an odd number} \end{cases}$$

$Y = X + 1$, $q_{az}^{k} = 1$ if GCM a is in the position z for the ranking technique k and 0 otherwise, T – Number of GCMs, K–Number of Indicators.

3. Results

3.1 Initial Selection

In the initial selection step, the compatibility of simulated precipitations from all GCM ensembles in the CMIP5-DIAS database was tested against the observed precipitation from GPCP. The analysis region was selected by the boundaries between the longitudes of 76.5°E, 83.5°E and latitudes of 4.5°N and 12°N, centring the southwest region of the island and encompassing the ocean.

Figures 4 shows the graphical outputs of daily rainfall variation and Figure 5 shows the average monthly rainfall around Sri Lanka in the Indian Ocean, derived using the GPCP rainfall matrix pertaining to the period from 1979–2005, which were obtained from DIAS.

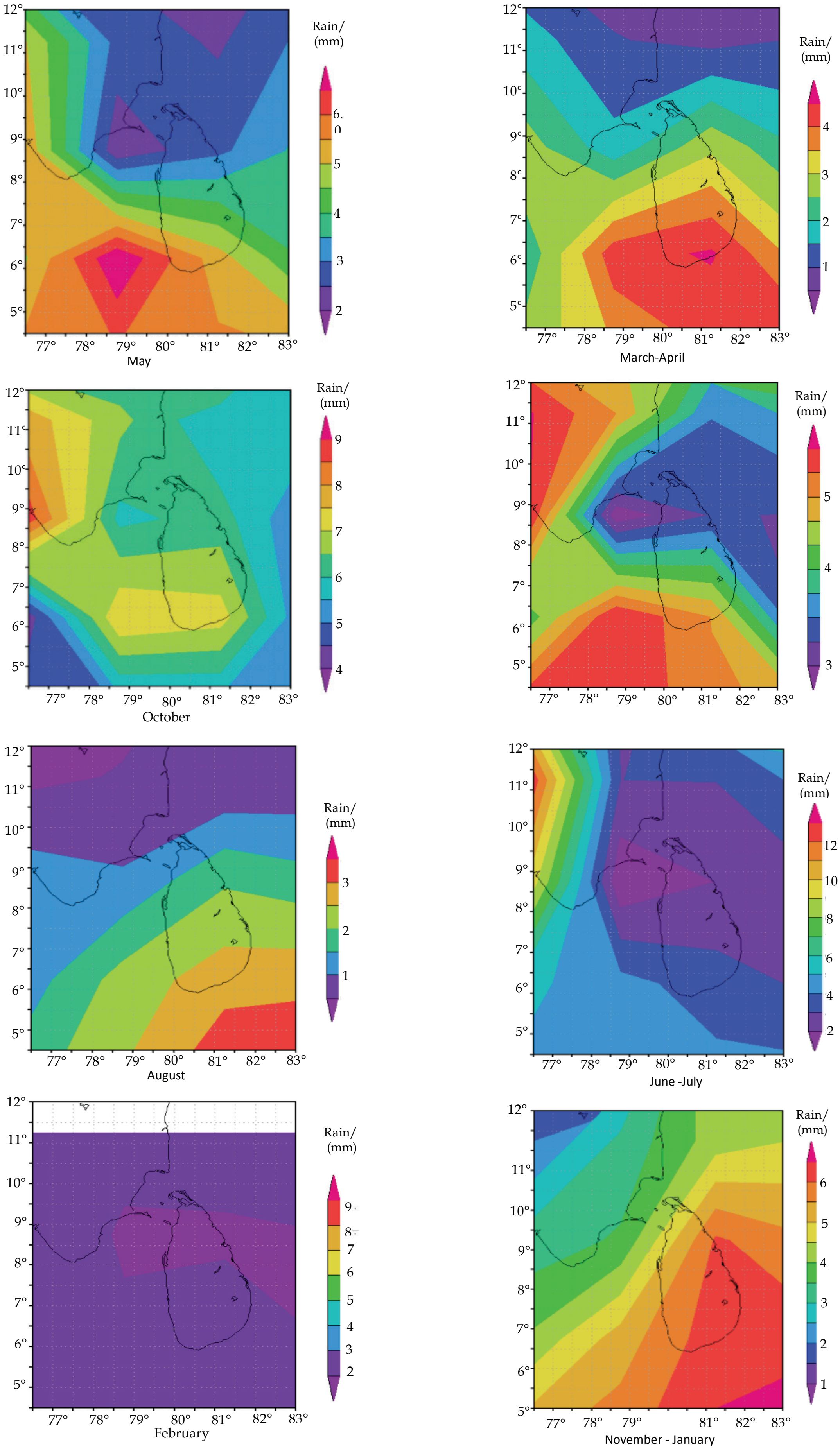

Figure 4 - Daily Rainfall Variation based on Time of the Year

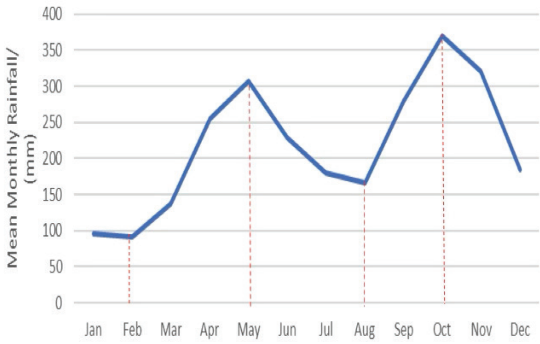

Figure 5 - Average Monthly Rainfall of the Southwest Region

Based on the above results, it is observed that during the first inter-monsoon period (March–April), the average daily rainfall is between 4 and 4.5 mm, and in September, which is the last month of the Southwest monsoon, it is 4.8–5.1 mm. During June and July, the average daily rainfall stays between 3 and 4 mm, and in the period from November to January, this increases to 5 and 6 mm. November is one of the two months in the second inter-monsoon and is likely to have higher rainfall.

During the Northeast monsoon from December to February, the Kalu Ganga catchment receives less rainfall. Therefore, it can be observed that the 6 mm average daily rainfall from November to January has been heavily contributed by the rainfall during November because of the second inter-monsoon. The same pattern has been identified by previous studies, with peaks in May and October and minima in February and August. However, in some rainfall stations, the May peak was observed to be higher than the October peak, in contrast to the results of other studies [5]. GPCP-gridded rainfall may include rainfalls outside the catchment boundary, as the resolution is coarser.

3.1.1 Ranking of GCMs based on Performance

The tests were conducted for eight different monthly rainfall configurations using two statistical performance indicators: RMSE and Scorr. The results of the initial selection are presented in Table 6 which is given in the Appendix. Following the allocation of marks in the initial analysis, the range of marks that a GCM could obtain was between -4 and 8. A GCM with a total mark closer to -4 would be unfavourable for modelling the monsoonal rainfall pattern, whereas a GCM with a total mark closer to 8 would be a preferable choice. The range of marks that a GCM could obtain is 12, and the percentage for passing a GCM through to the fine selection was set discretionarily at 25%, i.e., GCMs with at least a score of 3 were selected.

One GCM could have different ensembles based on various conditions. The initial selection was performed on each GCM ensemble, which allowed a greater number of GCM ensembles to be tested for compliance. Among all the ensembles tested in the Initial Selection step, the GCMs with ensemble r1i1p1 showed more compatibility as given in Table 6. Therefore, it was selected as the common ensemble for further analysis in the Fine Selection. Some of the GCMs that had no, or partial, rainfall data based on future scenarios were not selected for the Fine Selection to avoid the selection of GCMs with no or limited capability for further analysis [7,29], i.e., though CanCM4 obtained the highest marks, showing the best compatibility among all the other GCMs, it did not hold daily precipitation data for RCP 8.5 for the future scenario.

3.2 Fine Selection

Figure 6 shows the variation of mean monthly precipitation from 1962–2007 at the six selected grid locations under the Fine Selection step, based on APHRODITE. The variation of APHRODITE rainfalls is also similar to the GPCP variation shown in Figure 4.

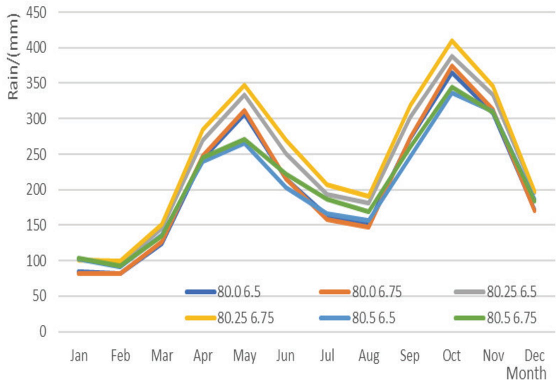

Figure 6 - Monthly Rainfall Variation at APHRODITE Coordinates

It is observed that the grid locations 80.25, 6.5 and 80.25, 6.75, which are located downstream of the Kalu Ganga, have the highest average monthly rainfall throughout the year, while the grid locations 80.5, 6.5 and 80.5, 6.75, located upstream, have the lowest values with respect to the peak rainfall of the catchment. For these upstream locations of the Kalu Ganga, which are above Ratnapura and closer to the central mountains, rainfall station data [19] indicate a higher rainfall reception compared to the downstream areas. However, the APHRODITE rainfall peaks show the opposite pattern, and a similar scenario has been observed for rainfall locations in Pakistan [4], where the APHRODITE data underestimate observed precipitation—especially in locations with higher rainfall peaks—while a slight overestimation has been noted for locations with lower rainfall. A similar characteristic of the APHRODITE data has also been found in [31], where the bias upstream is small and larger in the floodplains. Therefore, to overcome these inherent weaknesses, and depending on the monthly variations in APHRODITE data, the average rainfall for the total catchment was taken for the forthcoming analysis.

3.2.1 Analysis of GCMs' Performance

The Fine Selection is expected to provide better screening at the catchment scale in order to identify suitable GCMs that can simulate basin-scale precipitation variations. This also indicates which GCM simulations perform well after downscaling to the catchment level. Seven GCMs filtered in the initial selection were carried through to the Fine Selection under three categories: ERE, MWDR, and NRD. A total of six performance indicators were used for the statistical analysis in the Fine Selection process for the analyses of ERE, MWDR, and NRD. The calculated indicators under all three categories are tabulated in Tables 1 to 3.

NRMSD, ANMBD, AARD, and NSE are measures of deviation, with the lower margin being the ideal value for all except NSE. The ideal values for CC and SS are those with the highest values.

Referring to Table 1, CanESM2 has achieved the ideal values for NRMSD, ANMBD, AARD, and SS—four out of the five tested PIs. This shows that CanESM2 would be the most favourable GCM among the rest for simulating ERE. The ideal value for CC was obtained by CCSM4, and one of the other GCMs were able to secure an ideal value for any of the indicators. However, the normalized weightage of CC and SS is quite smaller relative to the others, which makes these two PIs incapable of affecting the decision-making process. The NSE figures for ERE contained both positive and negative values; hence, it was not used to calculate weightages.

Referring to Table 2, CESM1 (CAP) secured the ideal values for NRMSD, AARD, and NSE, while CNRM-CM5 secured ideal values for ANMBD, CC, and SS, although CNRM-CM5 showed an anti-ideal solution for AARD. However, the weightages of NRMSD, AARD, and SS are negligible compared to the others. CNRM-CM5 securing ideal values for ANMBD and CC accounts for a total weightage of 69%, while CESM1 (CAP), having an ideal value for NSE, has a weightage of 27%. This made the decision-making process a little difficult but more favourable to CNRM-CM5. It is worthy to note that the most favourable GCM selected for ERE, i.e., CanESM2, has shown anti-ideal solutions against all PIs except for AARD under the MWDR. This indicates that one GCM cannot perform well for all rainfall patterns.

Referring to Table 3, CanESM2 secured ideal values for NRMSD, NSE, and SS, while CNRM-CM5 and CCSM4 secured ideal values for AARD and CC, respectively. GFDL-ESM2M has anti-ideal values for all PIs except CC, which has been obtained by GFDL-ESM2G. The highest weightage of 71% among the PIs is held by NSE, and the ideal value for NSE has been obtained by CanESM2, which indicates that CanESM2 would be a better GCM for modelling the NRD.

3.2.2 Ranking of GCM based on Performance

When the performance of GCMs is evaluated, any single GCM has not secured the ideal solution under all PI rather it is observed that under each subcategory of fine selection, different GCMs have performed in a varied manner. Therefore, a further statistical test was carried out to conclude based on the observational results given above. Accordingly, compromise programming (LP_a) and TOPSIS were adopted in the study to evaluate and rank the GCMs according to their performance. The ranks that GCMs obtained based on the above two MCDM techniques are given in the Table 4. It is seen that both the ranking methods have given similar ranks under ERE and MWDR rainfall categories.

3.2.3 Group Decision Making - Net Strength (NSa) Values

Although the ranking techniques above gave similar rankings to each other, the Net Strength (NSa) values were calculated as outlined in the methodology. NSa is the difference between the total strength and the weakness of a GCM estimated relative to its rank under different ranking criteria. The different NSa values obtained by each GCM under the three subcategories of Fine Selection (ERE, MWDR, and NDD) are summarized in Table 5.

After analysing the results, it was observed that distinct GCMs obtained different NS_a values. The higher the NS_a, the more it indicates a suitable GCM for the purpose. In the event of extreme rainfall, CanESM2 had the highest net strength of 12, and CESM1 (BGC) was the runner-up with a score of 9. For MWDR, CNRM-CM5 obtained the highest NS_a value and is the best GCM to model monthly rainfalls. For NRD, both CNRM-CM5 and CanESM2 have obtained the highest NS_a values and hence either of the GCMs can be selected for modelling future Number of Dry Days.

Table 1 - PI Values under ERE Analysis

GCM	NRMSD	ANMBD	AARD	CC	SS
CanESM2	0.088	0.025	0.039	0.952	0.851
CESM1(BGC)	0.201	0.105	0.086	0.967	0.865
CESM1(CAP)	0.483	0.200	0.156	0.965	0.784
CNRM-CM5	0.516	0.411	0.375	0.948	0.554
CCSM4	0.220	0.126	0.106	0.976	0.824
GFDL-ESM2G	0.468	0.300	0.253	0.957	0.716
GFDL-SM2M	0.605	0.371	0.309	0.928	0.689
Normalized Weight	24.6%	38.1%	35.6%	0%	1.7%

Table 2 - PI Values under MWDR Analysis

GCM	NRMSD	ANMBD	AARD	CC	NSE	SS
CanESM2	0.7714	0.4333	0.8295	0.0895	-0.9895	0.6083
CESM1(BGC)	0.6669	0.0895	0.8601	0.2691	-0.4868	0.8208
CESM1(CAP)	0.6111	0.2703	0.6727	0.2982	-0.2486	0.7000
CNRM-CM5	0.6595	0.0318	0.9983	0.2619	-0.4541	0.8583
CCSM4	0.6571	0.2749	0.8277	0.2659	-0.4435	0.7458
GFDL-ESM2G	0.6979	0.3958	0.7726	0.2946	-0.6286	0.6958
GFDL-SM2M	0.6309	0.2539	0.7183	0.3001	-0.3306	0.6667
Normalized Weight	0.8%	54.4%	2.2%	14.1%	26.7%	1.9%

Table 3 - PI Values under NRD Analysis

GCM	NRMSD	AARD	CC	NSE	SS
CanESM2	0.5056	0.5869	0.2926	-0.5629	0.9208
CESM1(BCG)	0.5837	0.6541	0.3144	-1.0835	0.7375
CESM1(CAP)	0.5422	0.6035	0.2727	-0.7978	0.8958
CNRM-CM5	0.5058	0.5852	0.3053	-0.5644	0.8750
CCSM4	0.5823	0.6000	0.3185	-1.0734	0.7333
GFDL-ESM2G	0.6540	0.7302	0.1844	-1.6153	0.7042
GFDL-ESM2M	0.7087	0.7877	0.1906	-2.0715	0.6458
Normalized Weight	4.9%	4.3%	14.2%	71.2%	5.5%

Table 4 - Rankings of GCMs under different MCDM Techniques

GCM	ERE		MWDR		NRD	
	LP	TOPSIS	LP	TOPSIS	LP	TOPSIS
CanESM2	1	1	7	7	2	1
CESM1(BCG)	2	2	2	2	5	5
CESM1(CAP)	4	4	4	4	3	3
CNRM-CM5	7	7	1	1	1	2
CSM4	3	3	5	5	4	4
GFDL-2G	5	5	6	6	6	6
GFDL-2M	6	6	3	3	7	7

Table 5 - NSa Values of GCMs

GCM	NS_a		
	ERE	MWDR	NRD
CanESM2	12	-6	7
CESM1(BGC)	9	6	-2
CESM1(CAP)	3	3	4
CNRM-CM5	-8	8	7
CCSM4	6	-2	3
GFDL-ESM2G	-3	-4	-4
GFDL-ESM2M	-7	3	-6

4. Conclusion

The outcomes of climate-related studies using GCM projections potentially carry uncertainty because they rely on models developed based on many geophysical assumptions and boundaries. Previous studies identified uncertainty about future climate change impacts over the Kalu Ganga catchment due to different GCMs providing varied hydrological projections [34]. However, GCMs are effective tools for modelling future climate, and hence this study attempted to reduce the uncertainty of different GCM projections in the Kalu Ganga catchment by introducing a statistical approach to select appropriate GCM(s) capable of simulating future precipitation based on CMIP-5 outputs.

The GCMs were evaluated based on their performance by analysing simulated past rainfall against observed data under two selection stages. The Initial Selection identified potential GCMs that could model the southwest monsoonal climate using a larger domain consisting of ocean and land rainfall data, where the observed data were taken from the GPCP. Two performance indicators (PIs) were used to compare the monthly rainfall patterns in the southwest of Sri Lanka and screened 17 GCMs from the CMIP-5 database; of these, 7 GCMs progressed to the next stage, while the remaining GCMs were excluded due to constraints listed in Table 6.The Fine Selection analysed the performance of these 7 GCMs at the catchment scale after bias-correcting the GCM outputs under three different rainfall scenarios: Extreme Rainfall Events (ERE), Monthly Wet Day Rainfalls (MWDR), and No Rain Days (NRD), where observed precipitation was taken from APHRODITE. Six PIs were used to evaluate GCM performance, and MCDM techniques were employed to reach a final decision.

The results of the Fine Selection indicated that no single GCM could model all three rainfall categories with the same confidence level. CanESM2 was effective for extreme rainfall, CNRM-CM5 for normal rainfall, and both CanESM2 and CNRM-CM5 for no rain days. Through the study outcomes, CanESM2 appeared to be the better GCM for the region in terms of modelling tail rainfalls, such as extreme and no rain days, whereas CNRM-CM5 was more ideal for modelling normal rainfall. Some studies have identified that CNRM-CM5 performs well in simulating rainfall over land [13]. However, none of the GCMs selected in this study matched previous selections that used CMIP4 outputs [20], although CanESM2 and CNRM-CM5 were also found to perform well in the local context by previous studies [25]. Further comparison of this study's results with previous ones is difficult due to the limited number of studies on GCM selection in local catchments.

The developed method for GCM selection and bias correction for the Kalu Ganga basin used gridded precipitation data and statistical methods. The use of gridded precipitation data facilitated the analysis. However, the APHRODITE rainfall data is derived from available ground station data and therefore depends on the density of the rain-gauge network and the accuracy of primary data in the catchment of interest. APHRODITE data could underestimate actual rainfall [2], and future studies using satellite reanalysis data could verify this with observed data if available. The GCM selection method applied here, if adapted, can be deployed for other river basins as well. It is suggested for future studies to examine the possibility of integrating a greater number of rain gauge locations into the gridded rainfall matrices.

This study was primarily based on selecting GCMs to model future rainfall and no other climatic parameters. Hence, the only variable considered was rainfall, although many other geophysical attributes can govern GCM performance when selecting a suitable model [20]. Therefore, selecting GCMs based on their ability to reproduce past rainfall may not be suitable for broader climate change impact studies. However, introducing a simpler GCM selection method was a key feature of this study; thus, rainfall was the sole variable used, with statistical means employed to compare performance. The GCMs and their outputs in this study were based on CMIP-5; however, a newer database, CMIP-6, has since been introduced, including updated GCMs with higher climate sensitivity. Nevertheless, it remains a research question how much these new CMIP GCMs contribute to climate modelling in the South Asian region, where most GCMs are developed elsewhere.

The study focused on developing a low-cost data solution for GCM selection, and the applied methodology could be adapted for any other catchment of interest. Furthermore, the authors aimed to avoid the extra cost and inefficiency of acquiring primary data requiring additional funding, while APHRODITE has already compiled these primary data from the Meteorological Department of Sri Lanka and developed gridded data that other researchers can easily access online.

References

1. Adler, R. F., Huffman, G. J., Chang, A., Ferraro, R., Xie, P.-P., Janowiak, J., Rudolf, B., Schneider, U., Curtis, S., Bolvin, D., Gruber, A., Susskind, J., Arkin, P. and Nelkin, E., "The Version-2 Global Precipitation Climatology Project (GPCP) Monthly Precipitation Analysis (1979–Present)", *Journal of Hydrometeorology*, Vol. 4, No. 6, 2003.
2. Ahmed, K., Sachindra, D. A., Shahid, S., Iqbal, Z., Nawaz, N. and Khan, N., "Multi-Model Ensemble Predictions of Precipitation and Temperature Using Machine Learning Algorithms", *Atmospheric Research*, Vol. 236, 2020, p. 104806.
3. Alahacoon, N., Karthikeyan, M., Peejush, P. and Giriraj, A., "A Decadal Historical Satellite Data and Rainfall Trend Analysis (2001–2016) for Flood Hazard Mapping in Sri Lanka", *Remote Sensing*, Vol. 10, No. 3, 2018, p. 448.
4. Ali, G., Rasul, G., Mahmood, T., Zaman, Q. and Cheema, S. H., "Validation of APHRODITE Precipitation Data for Humid and Sub Humid Regions of Pakistan", *Pakistan Journal of Meteorology*, 2012.
5. Ampitiyawatta, A. and Guo, S., "Precipitation Trends in the Kalu Ganga Basin in Sri Lanka", *Journal of Agricultural Sciences*, Vol. 4, No. 1, 2010, pp. 10.
6. Burt, T. and Weerasinghe, K., "Rainfall Distributions in Sri Lanka in Time and Space: An Analysis Based on Daily Rainfall Data", *Climate*, Vol. 2, No. 4, 2014, pp. 242–263.
7. Chen, L. and Frauenfeld, O. W., "A Comprehensive Evaluation of Precipitation Simulations over China Based on CMIP5 Multimodel Ensemble Projections", *Journal of Geophysical Research: Atmospheres*, Vol. 119, No. 10, 2014, pp. 5767–5786.
8. Dissanayaka, K. D. C. R. and Rajapakse, R. L. H. L., "Long-Term Precipitation Trends and Climate Extremes in the Kelani River Basin, Sri Lanka, and Their Impact on Streamflow Variability under Climate Change", *Paddy and Water Environment*, Vol. 17, No. 2, 2019, pp. 281–289.
9. Edirisooriya, K. V. D., Vitanage, N. S., Uluwaduge, P. and Senevirathna, E. M. T. K., "Understanding Disaster Risk and Mitigation Special Reference to Ratnapura District", *Procedia Engineering*, Vol. 212, 2018, pp. 1034–1039.
10. Feigenwinter, I., Kotlarski, S., Casanueva, A., Schwierz, C. and Liniger, M. A., "Exploring Quantile Mapping as a Tool to Produce User-Tailored Climate Scenarios for Switzerland", *MeteoSchweiz*, 2018.
11. Hassan, I., Kalin, R. M., White, C. J. and Aladejana, J. A., "Selection of CMIP5 GCM Ensemble for the Projection of Spatio-Temporal Changes in Precipitation and Temperature over the Niger Delta, Nigeria", *Water*, Vol. 12, No. 2, 2020, p. 385.
12. Husak, G. J., Michaelsen, J. and Funk, C., "Use of the Gamma Distribution to Represent Monthly Rainfall in Africa for Drought Monitoring Applications", *International Journal of Climatology*, Vol. 27, No. 7, 2007, pp. 935–944.
13. Kamworapan, S. and Surussavadee, C., "Evaluation of CMIP5 Global Climate Models for Simulating Climatological Temperature and Precipitation for Southeast Asia", *Advances in Meteorology*, Vol. 2019, 2019, pp. 1–18.
14. Khan, A. and Koch, M., "Selecting and Downscaling a Set of Climate Models for Projecting Climatic Change for Impact Assessment in the Upper Indus Basin (UIB)", *Climate*, Vol. 6, No. 4, 2018, p. 89.
15. Lafon, T., Dadson, S., Buys, G. and Prudhomme, C., "Bias Correction of Daily Precipitation Simulated by a Regional Climate Model: A Comparison of Methods", *International Journal of Climatology*, Vol. 33, No. 6, 2012, pp. 1367–1381.
16. Li, H., Sheffield, J. and Wood, E. F., "Bias Correction of Monthly Precipitation and Temperature Fields from Intergovernmental Panel on Climate Change AR4 Models Using Equidistant Quantile Matching", *Journal of Geophysical Research*, Vol. 115, No. D10, 2010.
17. Lutz, A. F., ter Maat, H. W., Biemans, H., Shrestha, A. B., Wester, P. and Immerzeel, W. W., "Selecting Representative Climate Models for Climate Change Impact Studies: An Advanced Envelope-Based Selection Approach", *International Journal of Climatology*, Vol. 36, No. 12, 2016, pp. 3988–4005.
18. Martinez-Villalobos, C. and Neelin, J. D., "Why Do Precipitation Intensities Tend to Follow Gamma Distributions?", *Journal of the Atmospheric Sciences*, Vol. 76, No. 11, 2019, pp. 3611–3631.
19. Nandalal, K. D. W., "Use of a Hydrodynamic Model to Forecast Floods of Kalu River in Sri Lanka", *Journal of Flood Risk Management*, Vol. 2, No. 3, 2009, pp. 151–158.
20. Nyunt, C. T., Koike, T. and Yamamoto, A., "Statistical Bias Correction for Climate Change Impact on the Basin Scale Precipitation in Sri Lanka, Philippines, Japan and Tunisia", *Hydrology and Earth System Sciences Discussions*, 2016, pp. 1–32.
21. Nyunt, C. T., Yamamoto, H., Yamamoto, A., Nemoto, T., Kitsuregawa, M. and Koike, T., "Application of Bias-Correction and Downscaling Method to Kalu Ganga Basin in Sri Lanka", *Journal*

of Japan Society of Civil Engineers, Ser. B1 (Hydraulic Engineering), Vol. 68, No. 4, 2012, pp. I_115–I_120.

22. Pattanayak, S., "Attribution of Seasonal Temperature Changes in Sri Lanka to Anthropogenic and Natural Forcings Using CMIP5 Simulations", *Journal of Earth System Science*, Vol. 130, No. 2, 2021.
23. Ruan, Y., Yao, Z., Wang, R. and Liu, Z., "Ranking of CMIP5 GCM Skills in Simulating Observed Precipitation over the Lower Mekong Basin, Using an Improved Score-Based Method", *Water*, Vol. 10, No. 12, 2018, p. 1868.
24. Selvarajah, H., Koike, T., Rasmy, M., Tamakawa, K., Yamamoto, A., Kitsuregawa, M. and Zhou, L., "Development of an Integrated Approach for the Assessment of Climate Change Impacts on the Hydro-Meteorological Characteristics of the Mahaweli River Basin, Sri Lanka", *Water*, Vol. 13, No. 9, 2021, p. 1218.
25. Srinivasa Raju, K., Sonali, P. and Nagesh Kumar, D., "Ranking of CMIP5-Based Global Climate Models for India Using Compromise Programming", *Theoretical and Applied Climatology*, Vol. 128, No. 3–4, 2016, pp. 563–574.
26. Thevakaran, A., McGregor, J. L., Katzfey, J., Hoffmann, P., Suppiah, R. and Sonnadara, D. U. J., "An Assessment of CSIRO Conformal Cubic Atmospheric Model Simulations over Sri Lanka", *Climate Dynamics*, Vol. 46, No. 5–6, 2015, pp. 1861–1875.
27. Thevakaran, A., Suppiah, R. and Sonnadara, U., "Trends in Extreme Rainfall Events in Sri Lanka, 1961–2010", *Journal of the National Science Foundation of Sri Lanka*, Vol. 47, No. 3, 2019, p. 285.
28. Ahmed, K., Shahid, S., Wang, X., Nawaz, N. and Najeebullah, K., "Evaluation of Gridded Precipitation Datasets over Arid Regions of Pakistan", *Water*, Vol. 11, No. 2, 2019, p. 210.
29. Das, L., Akhter, J., Dutta, M. and Meher, J. K., "Ensemble-Based CMIP5 Simulations of Monsoon Rainfall and Temperature Changes Over South Asia", *Challenges in Agro-Environmental Research in Monsoon Asia*, 2015, pp. 41–60.
30. Emami, F. and Koch, M., "Evaluation of Statistical-Downscaling/Bias-Correction Methods to Predict Hydrologic Responses to Climate Change in the Zarrine River Basin, Iran", *Climate*, Vol. 6, No. 2, 2018, p. 30.
31. Ji, X., Li, Y., Luo, X., He, D., Guo, R., Wang, J., Bai, Y., Yue, C. and Liu, C., "Evaluation of Bias Correction Methods for APHRODITE Data to Improve Hydrologic Simulation in a Large Himalayan Basin", *Atmospheric Research*, 2020, p. 104964.
32. Kawasaki, A., Yamamoto, A., Koudelova, P., Acierto, R., Nemoto, T., Kitsuregawa, M. and Koike, T., "Data Integration and Analysis System (DIAS) Contributing to Climate Change Analysis and Disaster Risk Reduction", *Data Science Journal*, 2017.
33. Schulz, L. and Kingston, D. G., "GCM-Related Uncertainty in River Flow Projections at the Threshold for 'Dangerous' Climate Change: The Kalu Ganga River, Sri Lanka", *Hydrological Sciences Journal*, Vol. 62, No. 14, 2017, pp. 2369–2380.
34. Sengupta, A. and Rajeevan, M., "Uncertainty Quantification and Reliability Analysis of CMIP5 Projections for the Indian Summer Monsoon", *Current Science*, 2013.
35. Sharmila, S., Joseph, S., Sahai, A. K., Abhilash, S. and Chattopadhyay, R., "Future Projection of Indian Summer Monsoon Variability under Climate Change Scenario: An Assessment from CMIP5 Climate Models", *Global and Planetary Change*, Vol. 124, 2015, pp. 62–78.
36. Wickramagamage, P., "Spatial and Temporal Variation of Rainfall Trends of Sri Lanka", *Theoretical and Applied Climatology*, Vol. 125, No. 3–4, 2015, pp. 427–438.
37. Wilby, R. L. and Keenan, R., "Adapting to Flood Risk under Climate Change", *Progress in Physical Geography: Earth and Environment*, Vol. 36, No. 3, 2012, pp. 348–378.
38. Yatagai, A., Kamiguchi, K., Arakawa, O., Hamada, A., Yasutomi, N. and Kitoh, A., "APHRODITE: Constructing a Long-Term Gridded Precipitation Dataset for Asia Based on a Dense Network of Rain Gauges", *Bulletin of the American Meteorological Society (BAMS)*, 2012.
39. Opricovic, S. and Tzeng, G.-H., "Compromise Solution by MCDM Methods: A Comparative Analysis of VIKOR and TOPSIS", *European Journal of Operational Research*, Vol. 156, No. 2, 2004, pp. 445–455. https://doi.org/10.1016/s0377 2217(03)00020 .
40. IPCC, "Climate Change 2014: Synthesis Report", Contribution of Working Groups I, II and III to the Fifth Assessment Report of the Intergovernmental Panel on Climate Change, [Core Writing Team, R. K. Pachauri and L. A. Meyer (eds.)], IPCC, Geneva, Switzerland, 2014, 151 pp.
41. Romero, C. and Rehman, T., "Multiple Criteria Analysis for Agricultural Decisions", Second Edition, Elsevier, 2003.
42. De Silva, C. S., "Impacts of Climate Change on Water Resources in Sri Lanka", in *Sustainable Development of Water Resources, Water Supply and Environmental Sanitation: Proceedings of the 32nd WEDC International Conference*, Colombo, Sri Lanka, 13–17 November 2006, pp. 289–295.
43. Niroshinie, M. C., Babel, M. and Herath, S., "A Methodology to Analyze Extreme Flooding Under Future Climate Change Scenarios for Colombo", available at: https://www.semanticscholar.org (accessed 2021-07-01).

APPENDIX

Table 6. Initially Selected GCMs

No	Model	Ensemble	May	Oct	Feb	Aug	Mar-Apr	Jun-Jul	Sept	Nov-Jan	Sum	Data Availability
1	CanCM4	(r3i1p1)	1	0	1	1	1	1	1	1	7	No RCP 8.5 data
2	CanESM2	(r2i1p1)	1	-0.5	1	1	1	1	1	1	6.5	Available
3	CNRM-CM5-2	(r1i1p1)	1	1	1	0	1	1	1	0	6	No Daily data
4	CNRM-CM5	(r1i1p1)	1	0	1	0	1	1	1	1	6	Available
5	CESM1(CAM5)	(r3i1p1)	1	1	0	1	1	1	1	0	6	Available
6	EC-EARTH	(r14i1p1)	1	1	0	1	1	1	1	0	6	No RCP 8.5 data
7	CCSM4	(r1i1p1)	1	1	1	0	1	1	1	-0.5	5.5	Available
8	CESM1(WACCM)	(r2i1p1)	1	1	1	0	1	0	1	0	5	No Daily data
9	CESM1(FASTCHEM)	(r1i1p1)	1	1	1	0	0	1	1	-0.5	4.5	No RCP data
10	GFDL-ESM2G	(r1i1p1)	1	0	1	0	0	1	0	1	4	Available
11	GFDL-ESM2M	(r1i1p1)	1	0	1	0	0	1	0	1	4	Available
12	MIROC4h	(r2i1p1)	1	1	1	-0.5	1	-0.5	0	1	4	No RCP 8.5 data
13	CESM1(BGC)	(r1i1p1)	1	1	1	0	0	1	0	-0.5	3.5	Available
14	FGOALS-g2	(r5i1p1)	1	1	1	0	0	0	-0.5	1	3.5	Ensemble N/A
15	FIO-ESM	(r2i1p1)	1	1	1	-0.5	0	0	0	1	3.5	No Daily data
16	HadCM3	(r2i1p1)	-0.5	-0.5	1	1	-0.5	1	1	1	3.5	No RCP data
17	MIROC-ESM	(r3i1p1)	0	1	1	-0.5	1	0	0	1	3.5	Ensemble N/A